Article

Discovery Medicine 2026; 38(214): 3476–3489
https://doi.org/10.24976/Discov.Med.202638214.266

Targeting LTBP1 Attenuates Hypoxia-Induced Pulmonary Hypertension by Modulating Mitophagy

Xiaolan Zhang[1], Jiangwei Ni[2,*]

[1]Department of Pathology, The People's Hospital of Pingyang, 325400 Wenzhou, Zhejiang, China
[2]Department of Thoracic Surgery, The First Affiliated Hospital of Wenzhou Medical University, 325000 Wenzhou, Zhejiang, China
*Correspondence: drnjw666@163.com (Jiangwei Ni)
Submitted: 22 July 2026 Revised: 19 August 2026 Accepted: 15 September 2026 Published: 25 November 2026

Background: Pulmonary hypertension (PAH) is characterized by persistent structural alterations in the pulmonary vasculature, accompanied by right ventricular dysfunction, with mitochondrial dysfunction and dysregulated mitophagy emerging as key pathogenic mechanisms. Latent transforming growth factor-β binding protein 1 (LTBP1) has been implicated in extracellular matrix remodeling; however, its role in mitophagy and PAH progression remains unclear. This study aimed to investigate the role of LTBP1 in PAH and determine whether its effects are associated with mitophagy-related signaling.

Methods: Differentially expressed genes were screened based on the GSE117261 dataset to identify mitophagy-associated genes in PAH. For the animal experiments, hypoxia was used to induce a mouse model of PAH, followed by adeno-associated virus (AAV)-shRNA-mediated knockdown of LTBP1. Right ventricular function was assessed by echocardiography, and pulmonary vascular remodeling was evaluated by histological analysis. *In vitro*, pulmonary arterial smooth muscle cells (PASMCs) were exposed to hypoxic conditions following LTBP1 knockdown or corresponding control treatment. The proliferative, migratory, and apoptotic properties of PASMCs were evaluated by EdU incorporation, Transwell assays, and flow cytometry, respectively. Mitochondrial reactive oxygen species (ROS) and mitophagy-related protein expression were analyzed by MitoSOX staining and Western blotting. Rescue experiments were performed by overexpressing PTEN-induced putative kinase 1 (PINK1).

Results: A total of 24 shared candidates intersecting the differential expression profiles and mitophagy-related gene sets were identified, among which LTBP1 was significantly upregulated in PAH. Elevated LTBP1 expression was validated in hypoxia-exposed mouse lung tissues ($p < 0.05$). *In vivo* silencing of LTBP1 improved right ventricular function and attenuated pulmonary arterial remodeling ($p < 0.05$). Mechanistically, hypoxia induced mitochondrial ROS accumulation and activation of mitophagy-related proteins ($p < 0.05$), which were significantly reduced following LTBP1 knockdown ($p < 0.05$). In PASMCs, LTBP1 depletion inhibited proliferation and migration while promoting apoptosis under hypoxic conditions ($p < 0.05$). Notably, PINK1 overexpression partially reversed the impact of LTBP1 deficiency on PASMC dysfunction ($p < 0.05$).

Conclusions: LTBP1 is associated with PAH progression and may modulate mitophagy-related signaling, with its effects potentially involving mitochondrial ROS accumulation and PINK1/Parkin signaling, thereby promoting PASMC proliferation and migration. Targeting LTBP1 could serve as a potential therapeutic strategy for PAH.

Keywords: PAH; LTBP1; hypoxia; mitophagy; PINK1/Parkin pathway

Introduction

Pulmonary hypertension (PAH) is a severe cardiopulmonary disorder associated with substantial morbidity and mortality, characterized by sustained elevation of pulmonary arterial pressure, persistent remodeling of the pulmonary vasculature, and eventual right ventricular failure [1,2,3]. Although considerable advances have been made in the clinical management of PAH, its prognosis remains unfavorable, largely due to its complex and multifactorial pathogenesis and the lack of effective disease-modifying treatments [4,5]. A prominent pathological hallmark of PAH is the abnormal expansion and enhanced migratory activity of pulmonary arterial smooth muscle cells (PASMCs), accompanied by impaired apoptotic susceptibility [6,7], which collectively contribute to pulmonary vascular remodeling.

Growing evidence has highlighted mitochondrial dysfunction as a critical regulator of PAH progression [8,9,10]. Beyond serving as the main intracellular energy-generating organelles, mitochondria also function as central hubs for redox signaling and cell fate determination [11,12]. Under hypoxic conditions, disruption of mitochondrial homeostasis occurs, which in turn promotes excessive generation of reactive oxygen species (ROS) and induces the activation of adaptive mitochondrial quality-control processes, including mitophagy [13,14]. Mitophagy represents a selective autophagic mechanism that eliminates dysfunctional mitochondria and is predominantly regulated by the PINK1/Parkin signaling axis [15,16]. Although basal

Copyright: © 2026 The Author(s). Published by Discovery Medicine. This is an open access article under the CC BY 4.0 license.
Note: *Discovery Medicine* stays neutral with regard to jurisdictional claims in published maps and institutional affiliations.

mitophagy is essential for maintaining mitochondrial integrity, dysregulated or excessive mitophagy has been reported to contribute to abnormal PASMC proliferation and vascular remodeling in PAH [17,18]. However, the upstream molecular regulators governing mitophagy dysregulation in PAH remain incompletely understood.

Latent transforming growth factor-β binding protein 1 (LTBP1) is an extracellular matrix-associated glycoprotein that is essential for controlling the bioavailability and activation of transforming growth factor-β (TGF-β) [19,20]. LTBP1 has been extensively associated with multiple pathological processes, including tissue fibrosis, vascular remodeling, and extracellular matrix organization [21,22]. Recent studies have suggested that LTBP family proteins may participate in vascular remodeling processes; however, the precise contribution of LTBP1 to PAH, as well as its possible involvement in mitochondrial quality control, have not been defined. Importantly, emerging evidence supports a functional link between extracellular matrix alterations and mitochondrial dysfunction in vascular diseases [23,24], suggesting that LTBP1 may exert broader regulatory functions beyond extracellular matrix modulation.

Given this background, we hypothesized that LTBP1 may be involved in hypoxia-induced PAH through modulation of mitochondrial homeostasis and mitophagy. To address this hypothesis, bioinformatic analyses were combined with both animal and cell-based experimental models to characterize LTBP1 expression and elucidate its functional significance in PAH. Furthermore, we explored whether LTBP1 regulates PASMC biological behavior through the PINK1/Parkin-dependent mitophagy pathway. Our study seeks to advance our understanding of the molecular basis underlying PAH and to propose LTBP1 as a potential therapeutic target for mitigating hypoxia-driven pulmonary vascular remodeling.

Materials and Methods

Bioinformatics Analysis

Gene expression data were obtained from the Gene Expression Omnibus (GEO) database. The GSE117261 dataset, generated on the GPL6244 platform, was downloaded and analyzed to identify differentially expressed genes (DEGs) between PAH and control lung tissues [25]. The dataset comprised 83 human lung tissue samples, including 58 samples from patients with PAH and 25 control samples. PAH lung tissues were obtained at the time of transplantation from patients with end-stage PAH, whereas control lung tissues were obtained from donors whose lungs were not suitable for transplantation. Raw expression data were processed and normalized using the limma package implemented in R. DEGs were subsequently determined using the empirical Bayes method, applying an adjusted $p < 0.05$ and $|\log_2$ fold change (FC)$| > 1$ as the significance thresholds. Volcano plots and heatmaps were constructed with the ggplot2 and pheatmap packages, respectively. Mitophagy-related genes were systematically collected from the GeneCards database by searching the keyword “mitophagy”. Candidate mitophagy-related DEGs were identified by intersecting the DEGs with the mitophagy-related gene set using an online Venn diagram tool. The expression level of the candidate gene LTBP1 in the GSE117261 dataset was further extracted and compared between PAH and control samples.

Animal Experiments

All animal experiments were conducted at the Laboratory Animal Center of Wenzhou University and approved by the Animal Ethics and Welfare Committee of Wenzhou University (Approval No. WZU-2025-022). Male C57BL/6 mice (8 weeks old, 20–25 g) were obtained from Speifer Marine Biotechnology (Beijing, China). Mice were randomly assigned into two independent experimental cohorts. In the first cohort, mice were randomly assigned to two groups (n = 5 per group): Normoxia and Hypoxia. The Hypoxia group was subjected to normobaric hypoxia (10% O_2) for 8 h per day over a period of 5 weeks using a hypoxia chamber (ProOx P360 oxygen sensor, Biospherix, NY, USA), while the Normoxia group was maintained under ambient oxygen conditions (21% O_2) throughout the experimental period. In the second cohort, mice were randomly divided into four groups (n = 5 per group): Normoxia, Hypoxia, Hypoxia + AAV-shNC, and Hypoxia + AAV-shLTBP1. Mice in the hypoxia-related groups were subjected to the same hypoxic exposure protocol described above.

AAV9-Mediated LTBP1 Silencing

Recombinant adeno-associated virus serotype 9 carrying short hairpin RNA targeting LTBP1 (AAV-shLTBP1; target sequence: 5′-GCTACAGATGCTCCTGCAA-3′) and negative control (AAV-shNC; target sequence: 5′-TTCTCCGAACGTGTCACGT-3′) were purchased from GeneChem (Shanghai, China). Mice were injected via the tail vein with 1×10^{11} viral genomes (vg) in 100 µL sterile phosphate-buffered saline (PBS) 2 weeks prior to hypoxia exposure. At the end of the experimental period, mice were anesthetized with tribromoethanol (240 mg/kg, intraperitoneally; T48402, Sigma-Aldrich, MO, USA) using a 0.25% working solution (12.5 mg/mL) prepared by diluting the stock solution 1:80 with physiological saline. Mice in the second cohort underwent right ventricular systolic pressure (RVSP) measurement. After adequate anesthesia was confirmed by the absence of the pedal withdrawal reflex, RVSP was measured as described below. Following completion of the hemodynamic measurements, these mice were euthanized by cervical dislocation under deep anesthesia. Blood samples were collected, and lung and heart tissues were rapidly excised. Pulmonary arterioles were

carefully dissected from the lung tissues under a stereomicroscope. The degree of right ventricular (RV) hypertrophy was evaluated by calculating the RV/(LV+S) index, defined as the ratio of the weight of the RV free wall to the combined weight of the left ventricle (LV) and interventricular septum (S). For morphometric analysis, pulmonary arterial medial wall thickness was measured from histological images using ImageJ software (National Institutes of Health, Bethesda, MD, USA).

Echocardiography

Cardiac function was assessed using a high-resolution imaging system (Vevo 2100 Imaging System, VisualSonics, Toronto, Canada). Mice were anesthetized with tribromoethanol (250 mg/kg, intraperitoneally), and echocardiographic measurements were performed after a stable plane of anesthesia was achieved. Right ventricular parameters, including right ventricular ejection fraction (RVEF), right ventricular end-diastolic diameter (RVEDD), and tricuspid annular plane systolic excursion (TAPSE), were measured from parasternal long-axis and short-axis views.

RVSP Measurement

A polyethylene catheter prefilled with heparinized saline was connected to a pressure transducer (ADInstruments, Sydney, Australia) and inserted into the right ventricle via the right external jugular vein. Correct catheter placement was confirmed by the appearance of a characteristic right ventricular pressure waveform. After a stabilization period of approximately 5 min, pressure signals were continuously recorded using a PowerLab data acquisition system (ADInstruments, Sydney, Australia), and RVSP values were analyzed with LabChart software (ADInstruments). The final RVSP value for each animal was calculated as the average of multiple consecutive cardiac cycles.

Histological Analysis

Lung tissues were fixed in 4% paraformaldehyde, followed by paraffin embedding and sectioning at a thickness of 4 μm. Histopathological assessment was performed using hematoxylin and eosin (HE) with a commercial kit (C0105, Beyotime, Shanghai, China) and observed under a light microscope. For immunohistochemical analysis, paraffin-embedded lung sections underwent sequential deparaffinization and rehydration, followed by heat-mediated antigen retrieval using citrate buffer (pH 6.0). The tissue sections were subsequently blocked with 5% BSA and incubated at 4 °C overnight with primary antibodies targeting LTBP1 (1:50; 22065-1-AP, Proteintech, Wuhan, China) and LC3 (1:200; 14600-1-AP, Proteintech, Wuhan, China). HRP-conjugated secondary antibodies (1:10,000; RGAR011, Proteintech, Wuhan, China) were then applied, and immunoreactivity was visualized using DAB staining under a light microscope.

Cell Culture and Treatment

Human PASMCs (SNL-679) were purchased from SUNNCELL (Wuhan, China). Cells were cultured in Dulbecco's Modified Eagle Medium (DMEM; 11965-092, Gibco, NY, USA) supplemented with 10% fetal bovine serum (FBS; 10099141, Gibco, NY, USA) and 1% penicillin–streptomycin under standard conditions (37 °C, 5% CO_2). The identity of the PASMCs was authenticated by short tandem repeat (STR) profiling, and the cells were confirmed to be free of mycoplasma contamination by routine mycoplasma testing before use. For hypoxic conditions, cells were cultured in an incubator (Thermo Scientific, MA, USA) with 1% O_2, 5% CO_2, and 94% N_2 for 48 h.

Cell Transfection

Short hairpin RNA targeting LTBP1 (sh-LTBP1; target sequence: 5′-GCAAGGAGTCAAAGTGAAA-3′) and the corresponding negative control shRNA (sh-NC; target sequence: 5′-TTCTCCGAACGTGTCACGT-3′) were purchased from GenePharma (Shanghai, China). The PINK1 overexpression plasmid (oe-PINK1) was constructed by cloning the full-length coding sequence of human PINK1 (NM_032409.3) into an expression vector, and the recombinant plasmid was verified by sequencing. The empty vector was used as the negative control (oe-NC).

Cells were transfected with shRNA or plasmids using Lipofectamine 3000 (L3000001, Invitrogen, CA, USA) according to the manufacturer's instructions. Briefly, PASMCs were seeded into 6-well plates and transfected with sh-LTBP1 or sh-NC at a final concentration of 50 nM, or with oe-PINK1 and oe-NC plasmids at a concentration of 1 μg per well. After transfection for 6 h, the transfection mixture was discarded and replaced with fresh complete medium. Cells were then maintained for a further 48 h. Successful LTBP1 depletion and PINK1 upregulation were verified at both the mRNA and protein levels using quantitative PCR (qPCR) and Western blot analysis, respectively.

Proliferation Assay

Cell proliferation was assessed using the EdU assay kit (C0071, Beyotime, Shanghai, China). PASMCs were incubated with 20 μM EdU for 2 h, fixed with 4% paraformaldehyde, and stained according to the protocol. Nuclei were counterstained with DAPI. Images were captured using a fluorescence microscope (Zeiss, Oberkochen, Germany), and EdU-positive cells were quantified.

Migration Assay

Cell migration was evaluated using Transwell chambers (8 μm pore size). PASMCs (1×10^4 cells) were seeded in the upper chamber in serum-free medium, while the lower chamber contained medium with 10% FBS. After

24 h incubation under normoxic or hypoxic conditions, migrated cells were fixed, stained with 0.1% crystal violet, and counted under a microscope.

Apoptosis Assay

Apoptosis was assessed using an Annexin V-FITC/PI apoptosis detection kit (C1062, Beyotime, Shanghai, China). Cells were collected, washed with PBS, and stained with Annexin V-FITC and PI for 15 min in the dark. Samples were analyzed using flow cytometry (BD Biosciences, CA, USA).

Mitochondrial ROS Measurement

Mitochondrial ROS levels were measured using MitoSOX Red (M36005, Invitrogen, CA, USA). Cells were incubated with 5 μM MitoSOX for 10 min at 37 °C, and imaged using a fluorescence microscope. Fluorescence intensity was quantified using ImageJ software.

qPCR

Total RNA was extracted using TRIzol reagent (15596026, Invitrogen, CA, USA). cDNA was synthesized using a reverse transcription kit (RR047A, Takara, Shiga, Japan). qPCR was performed using SYBR Green Master Mix (RR820A, Takara) on a QuantStudio 6 system (Applied Biosystems, USA). Gene expression was normalized to GAPDH using the $2^{-\Delta\Delta Ct}$ method. Primer sequences are listed in Table 1.

Table 1. Primer sequences used in qPCR.

Genes	Primer sequences
LTBP1 (mouse)-F	TGCCTGTGGAAGTAGCTCCTGA
LTBP1 (mouse)-R	AGTGTCCTGCTCCGCAAATGTC
GAPDH (mouse)-F	CATCACTGCCACCCAGAAGACTG
GAPDH (mouse)-R	ATGCCAGTGAGCTTCCCGTTCAG
LTBP1 (human)-F	TGAATGCCAGCACCGTCATCTC
LTBP1 (human)-R	CTGGCAAACACTCTTGTCCTCC
PINK1 (human)-F	GTGGACCATCTGGTTCAACAGG
PINK1 (human)-R	GCAGCCAAAATCTGCGATCACC
GAPDH (human)-F	GTCTCCTCTGACTTCAACAGCG
GAPDH (human)-R	ACCACCCTGTTGCTGTAGCCAA

qPCR, quantitative PCR; *LTBP1*, latent transforming growth factor-β binding protein 1; *GAPDH*, glyceraldehyde-3-phosphate dehydrogenase; *PINK1*, PTEN-induced putative kinase 1.

Western Blotting

Proteins were extracted using RIPA lysis buffer (P0013B, Beyotime, Shanghai, China) supplemented with protease inhibitors. Equal amounts of protein were separated by SDS-PAGE and transferred to PVDF membranes. Membranes were incubated with primary antibodies against LTBP1 (1:500; 22065-1-AP, Proteintech, Wuhan, China), PINK1 (1:1000; 23274-1-AP, Proteintech, Wuhan, China), Parkin (1:1000; 14060-1-AP, Proteintech, Wuhan, China), LC3 (1:2000; 14600-1-AP, Proteintech, Wuhan, China), p62 (1:5000; 84826-1-RR, Proteintech, Wuhan, China) and β-actin (1:4000; 20536-1-AP, Proteintech, Wuhan, China), followed by HRP-conjugated secondary antibodies (1:2000; SA00001-2, Proteintech, Wuhan, China). Bands were visualized using ECL substrate and quantified using ImageJ.

Statistical Analysis

All data are presented as mean ± standard deviation (SD). The normality of data distribution was assessed using the Shapiro–Wilk test before statistical analysis. Statistical analysis was performed using GraphPad Prism 9.5 (GraphPad Software, CA, USA). Comparisons between two groups were performed using Student's *t*-test, and multiple group comparisons were analyzed using one-way ANOVA followed by Tukey's post hoc test. A value of $p < 0.05$ was considered statistically significant.

Results

LTBP1 Is Upregulated in PAH

To identify pivotal genes linked to mitophagy in PAH, differential expression profiling was conducted based on the GSE117261 dataset. A total of DEGs were identified and visualized by volcano plot and heatmap (Fig. 1A,B). By intersecting these DEGs with a curated set of mitophagy-related genes, 24 overlapping candidates were obtained (Fig. 1C). Among these candidates, LTBP1 was selected for further analysis based on previous evidence showing that LTBP1 is upregulated in PAH and pulmonary vascular remodeling and may serve as a potential diagnostic marker for PAH [26]. Expression profiling demonstrated that LTBP1 was significantly elevated in the PAH group compared with Con in the GSE117261 dataset ($p < 0.05$) (Fig. 1D). To validate this finding *in vivo*, immunoblotting showed a significant elevation of LTBP1 protein in the hypoxia group relative to the normoxia group ($p < 0.05$) (Fig. 1E,F), which was further supported by quantitative analysis. Consistently, qPCR results confirmed a significant elevation of LTBP1 mRNA expression under hypoxic conditions ($p < 0.05$) (Fig. 1G). In addition, immunohistochemical staining revealed enhanced LTBP1 expression in lungs of hypoxia-treated mice (Fig. 1H,I). These findings indicate that LTBP1 is markedly upregulated in PAH and may be closely linked to mitophagy-related regulatory mechanisms.

LTBP1 Deficiency Preserves Right Ventricular Structure and Function Under Hypoxic Stress

To explore the function of LTBP1 in hypoxia-induced cardiopulmonary injury, an *in vivo* loss-of-function approach was employed using AAV-shLTBP1. Efficient

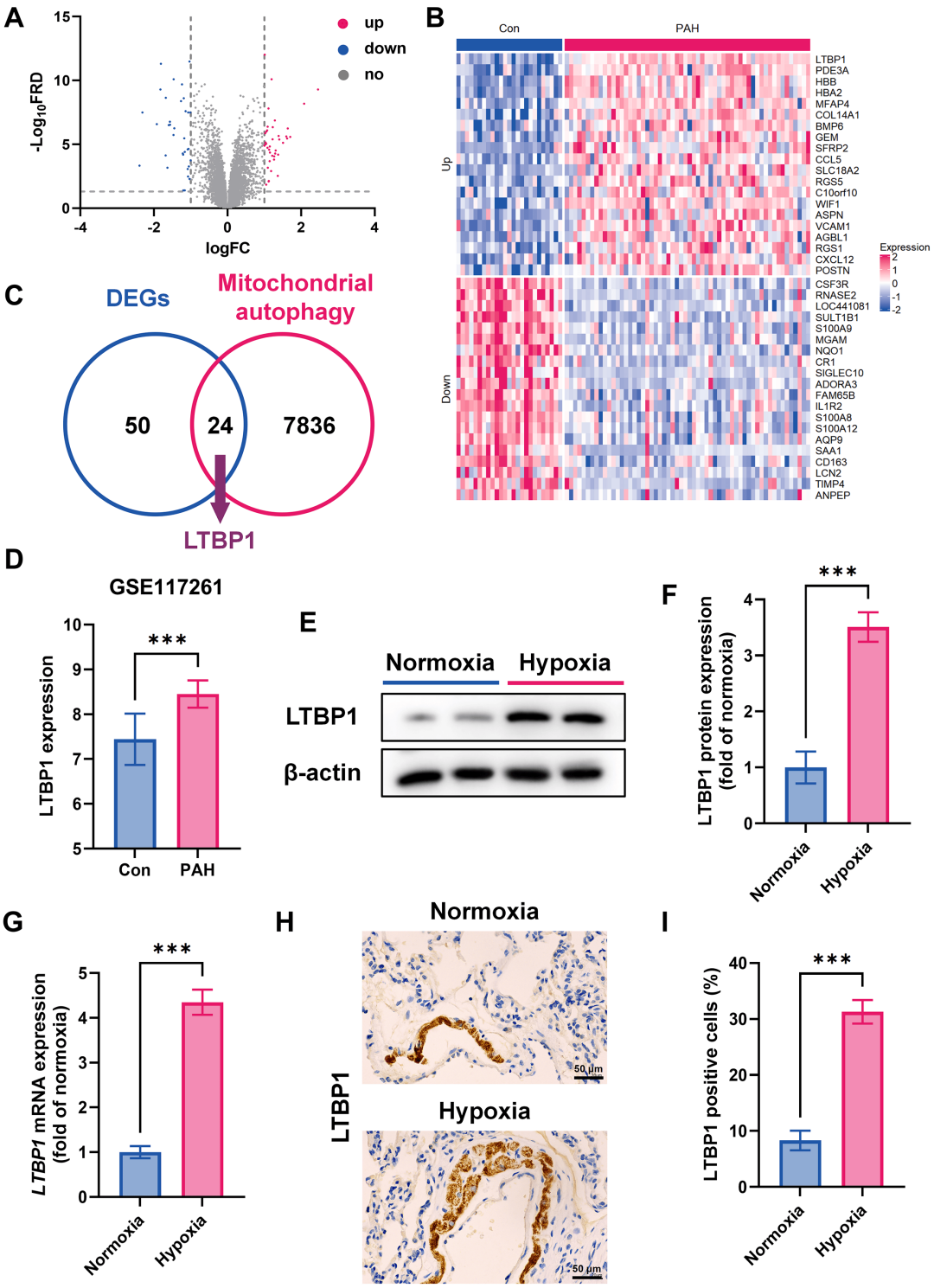


Fig. 1. Identification of LTBP1 as a mitophagy-associated gene in hypoxia-induced PAH. (A,B) Volcano plot and heatmap showing DEGs in the GSE117261 dataset. (C) Venn diagram showing the shared genes between DEGs and the mitophagy-related gene set. (D) LTBP1 expression profile in the GSE117261 dataset. (E,F) Representative immunoblotting results and densitometric evaluation of LTBP1 protein in lung tissues from normoxic and hypoxic mice. (G) qPCR analysis of LTBP1 mRNA expression. (H) Representative images of LTBP1 immunohistochemical staining in lung sections (scale bar: 50 μm). (I) Quantitative analysis of LTBP1-positive staining. n = 5 per group. ***$p < 0.001$. PAH, pulmonary hypertension; DEGs, differentially expressed genes.

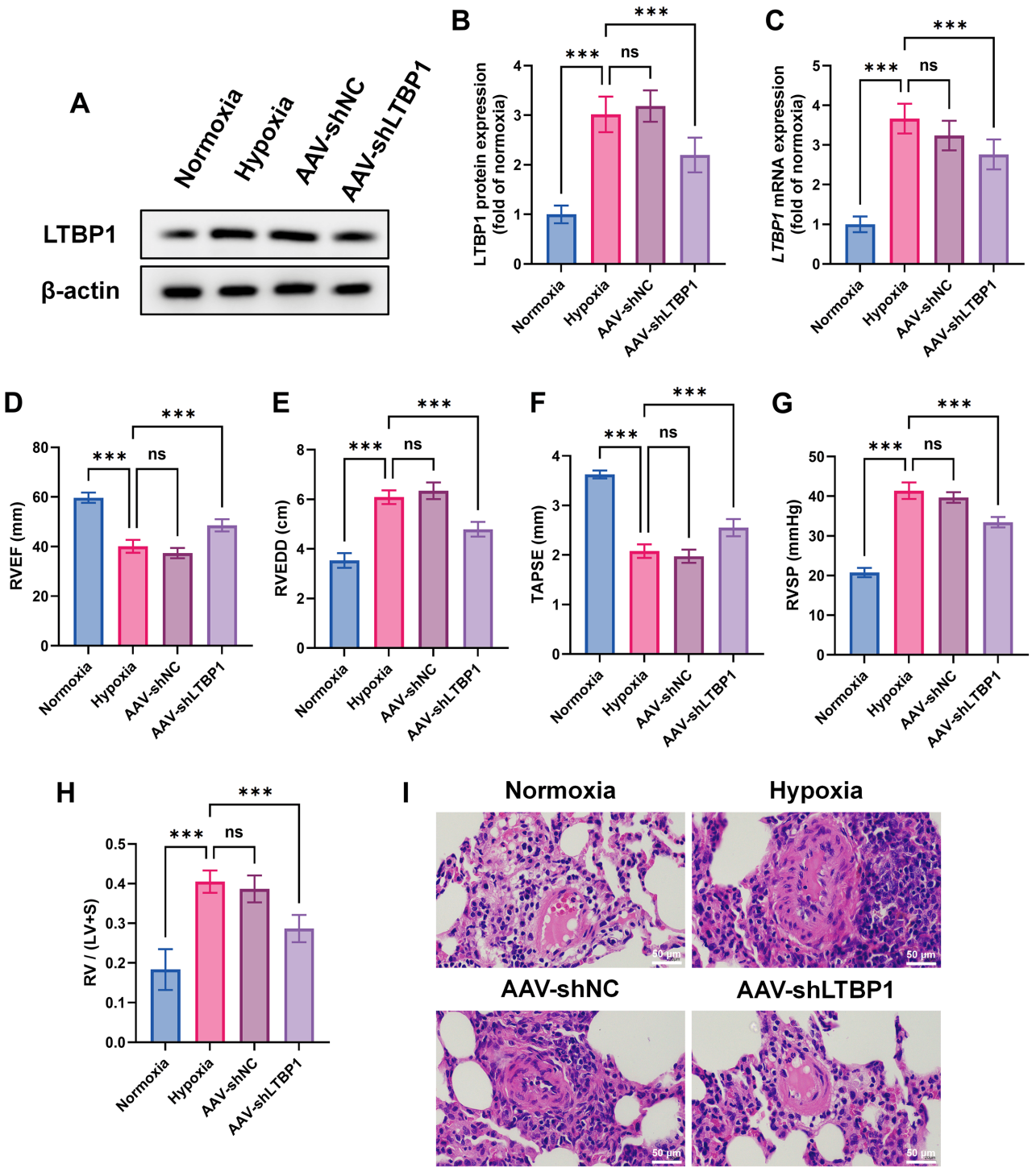


Fig. 2. *In vivo* silencing of LTBP1 attenuates hypoxia-induced right ventricular dysfunction. (A–C) Validation of AAV-shLTBP1–mediated knockdown at protein and mRNA levels. (D–F) Echocardiographic assessment of right ventricular function, including RVEF, RVEDD, and TAPSE. (G) Invasive hemodynamic assessment of RVSP. (H) Quantification of right ventricular hypertrophy by RV/(LV+S). (I) Representative H&E staining of lung tissue (scale bar: 50 μm). n = 5 per group. ns, no significant difference, ***$p <$ 0.001. AAV, adeno-associated virus; RVEF, right ventricular ejection fraction; RVEDD, right ventricular end-diastolic diameter; TAPSE, tricuspid annular plane systolic excursion; RVSP, right ventricular systolic pressure; LV, left ventricle; S, interventricular septum; H&E, hematoxylin and eosin.

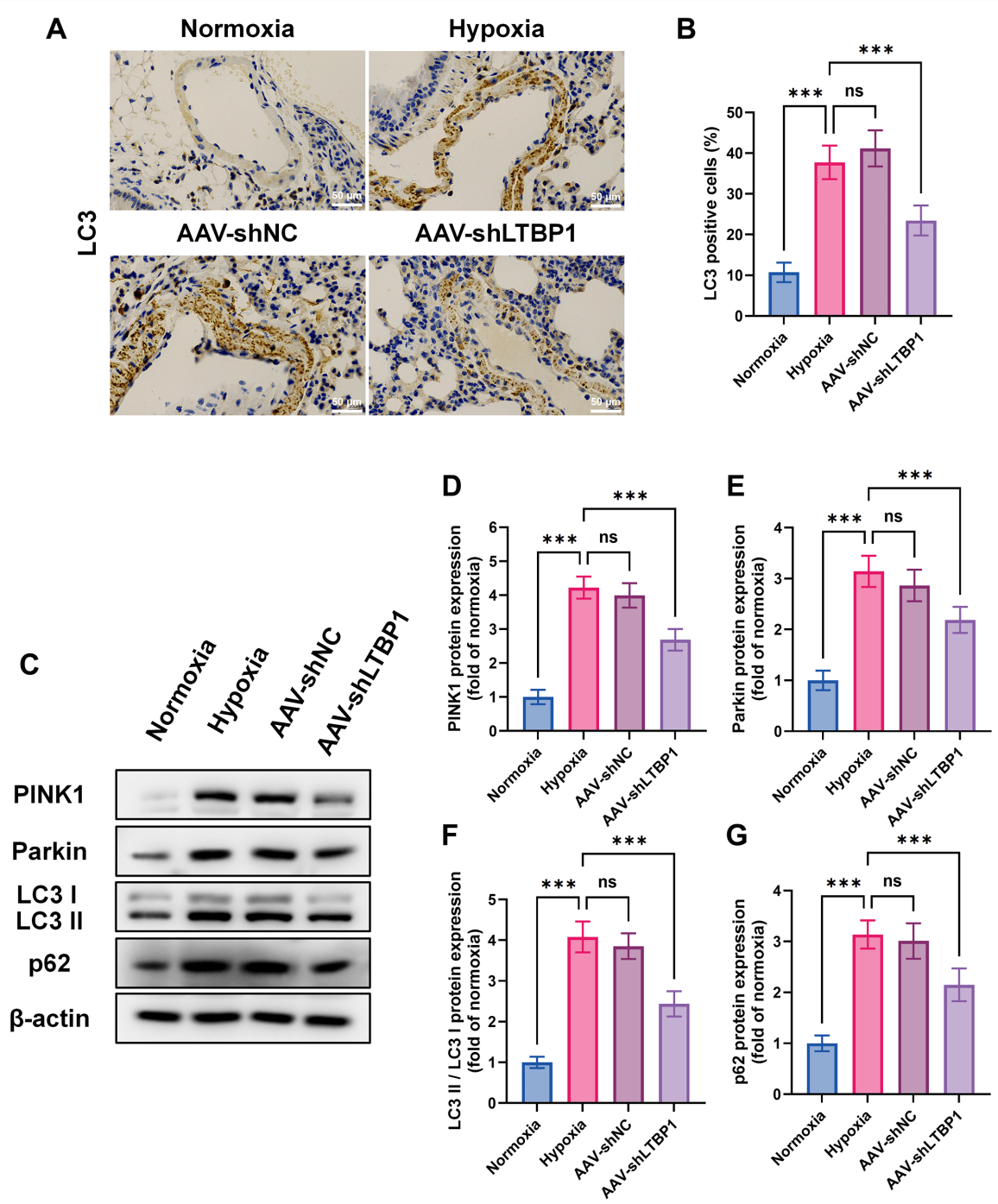


Fig. 3. LTBP1 modulates mitophagy-related signaling in lung tissue. (A) Immunohistochemical detection of LC3 expression (scale bar: 50 μm). (B) Quantitative analysis of LC3-positive staining. (C) Western blot analysis of mitophagy-related proteins. (D–G) Densitometric quantification of protein expression. n = 5 per group. ns, no significant difference, ***$p < 0.001$. LC3, microtubule-associated protein 1 light chain 3.

knockdown of LTBP1 was confirmed at both the protein and mRNA levels. As expected, LTBP1 expression was markedly elevated in the Hypoxia and AAV-shNC groups, whereas AAV-shLTBP1 treatment significantly reduced its expression, although levels remained higher than those observed under normoxic conditions ($p < 0.05$) (Fig. 2A–C). Cardiac function was subsequently evaluated by echocardiography. Hypoxia exposure led to a pronounced decline in RVEF and TAPSE, accompanied by increases in RVEDD, indicating substantial right ventricular dysfunction ($p < 0.05$) (Fig. 2D–F). Invasive hemodynamic assessment revealed a significant increase in RVSP following hypoxia exposure ($p < 0.05$) (Fig. 2G). In contrast, LTBP1 knockdown significantly improved right ventricular perfor-

mance, as evidenced by increased RVEF and TAPSE, together with reduced RVEDD and RVSP. Consistently, assessment of right ventricular hypertrophy revealed a significant increase in the RV/(LV+S) ratio in the Hypoxia and AAV-shNC groups compared with Normoxia, whereas AAV-shLTBP1 treatment markedly attenuated this effect ($p < 0.05$) (Fig. 2H). H&E staining provided additional histological evidence. Specifically, examination of pulmonary arterial structures revealed that hypoxia exposure induced significant thickening of the arterial wall and luminal narrowing. In contrast, these pathological alterations were markedly attenuated in the AAV-shLTBP1 group, with thinner arterial walls and partial restoration of luminal area (Fig. 2I). These findings indicate that suppression of LTBP1 effectively improves hypoxia-associated right ventricular dysfunction and attenuates cardiopulmonary remodeling.

LTBP1 Promotes Activation of Mitophagy Pathways in Hypoxia-Exposed Lung Tissue

To investigate the involvement of LTBP1 in mitophagy regulation *in vivo*, mitophagy-related markers were assessed in pulmonary tissues. Immunohistochemical analysis demonstrated that LC3 expression was markedly increased in the Hypoxia and AAV-shNC groups (Fig. 3A,B). Notably, this elevation was significantly attenuated following LTBP1 knockdown, although LC3 expression remained elevated relative to normoxic controls. Western blotting demonstrated that mitophagy-associated markers, including PINK1, Parkin, and the LC3 II/I ratio, were significantly upregulated in the Hypoxia and AAV-shNC groups, while p62 expression was also increased (Fig. 3C), suggesting an overall activation of mitophagy-associated signaling. Importantly, LTBP1 knockdown markedly reduced these protein markers relative to the Hypoxia and AAV-shNC conditions. Densitometric quantification further confirmed these trends ($p < 0.05$) (Fig. 3D–G), demonstrating that LTBP1 knockdown partially reversed hypoxia-induced activation of mitophagy-related pathways. These data support a role for LTBP1 in promoting mitophagy-associated signaling in hypoxic lung tissue.

LTBP1 Facilitates PASMC Growth and Motility While Suppressing Apoptotic Responses Under Hypoxia

To further clarify the biological function of LTBP1 in PASMCs, an *in vitro* knockdown model was established under hypoxic conditions. Successful knockdown efficiency of LTBP1 was verified at both protein and transcript levels (Fig. 4A–C). Similar to the changes observed *in vivo*, hypoxic treatment increased LTBP1 expression in both the Hypoxia and sh-NC groups ($p < 0.05$), whereas silencing of LTBP1 significantly reduced. PASMC proliferative activity was evaluated by EdU incorporation assay (Fig. 4D,E). Hypoxia exposure significantly enhanced PASMC proliferative capacity, as indicated by an increased proportion of EdU-positive cells in the Hypoxia and sh-NC groups relative to Normoxia ($p < 0.05$). In contrast, LTBP1 knockdown markedly suppressed this hypoxia-induced proliferative response ($p < 0.05$). Similarly, Transwell assays showed that hypoxic exposure markedly enhanced the migratory capacity of PASMCs (Fig. 4F,G). Notably, depletion of LTBP1 substantially attenuated cell migration compared with the hypoxia-treated group ($p < 0.05$). In addition, flow cytometric analysis revealed that hypoxia markedly inhibited PASMC apoptosis (Fig. 4H,I), as indicated by a reduced apoptotic rate in the Hypoxia and sh-NC groups compared with Normoxia ($p < 0.05$). Importantly, LTBP1 knockdown significantly increased apoptosis under hypoxic conditions ($p < 0.05$). These results reveal that LTBP1 facilitates PASMC proliferative and migratory responses while inhibiting apoptosis, thereby contributing to the pathogenic cellular phenotype induced by hypoxia.

LTBP1 Drives Mitochondrial ROS Accumulation and Mitophagy-Associated Signaling in PASMCs Under Hypoxia

To explore the involvement of LTBP1 in mitochondrial homeostasis, mitochondrial ROS production and mitophagy-associated signaling were evaluated in PASMCs. MitoSOX staining revealed that hypoxia markedly increased mitochondrial ROS levels, as indicated by enhanced fluorescence intensity in the hypoxia group ($p < 0.05$) (Fig. 5A,B). Importantly, LTBP1 knockdown significantly attenuated this increase ($p < 0.05$). Western blotting indicated that hypoxia induced a significant upregulation of mitophagy-related proteins, including PINK1, Parkin, and the LC3 II/I ratio, along with increased p62 expression in the Hypoxia and sh-NC groups ($p < 0.05$) (Fig. 5C–G). Notably, silencing of LTBP1 markedly reduced the expression of these proteins ($p < 0.05$). These results suggest that LTBP1 is closely involved in regulating mitochondrial ROS production and mitophagy under hypoxic conditions.

To further explore the role of PINK1, a PINK1 overexpression model was established in normoxic PASMCs. The efficiency of PINK1 overexpression was verified (Fig. 5H–J), providing a basis for subsequent rescue experiments.

PINK1 Restoration Counteracts the Effects of LTBP1 Silencing on Mitophagy and PASMC Phenotypes

To further delineate the mechanistic link between LTBP1 and mitophagy, rescue experiments were performed by overexpressing PINK1 in LTBP1-silenced PASMCs under hypoxic conditions. Western blot analysis showed that PINK1 overexpression partially restored the levels of these mitophagy-related proteins, including PINK1, Parkin, the LC3 II/I ratio, and p62, with expression levels higher than those observed in the sh-LTBP1 group ($p < 0.05$) (Fig. 6A–E). Functional assays further supported these findings. EdU incorporation analysis demonstrated that PINK1 overex-

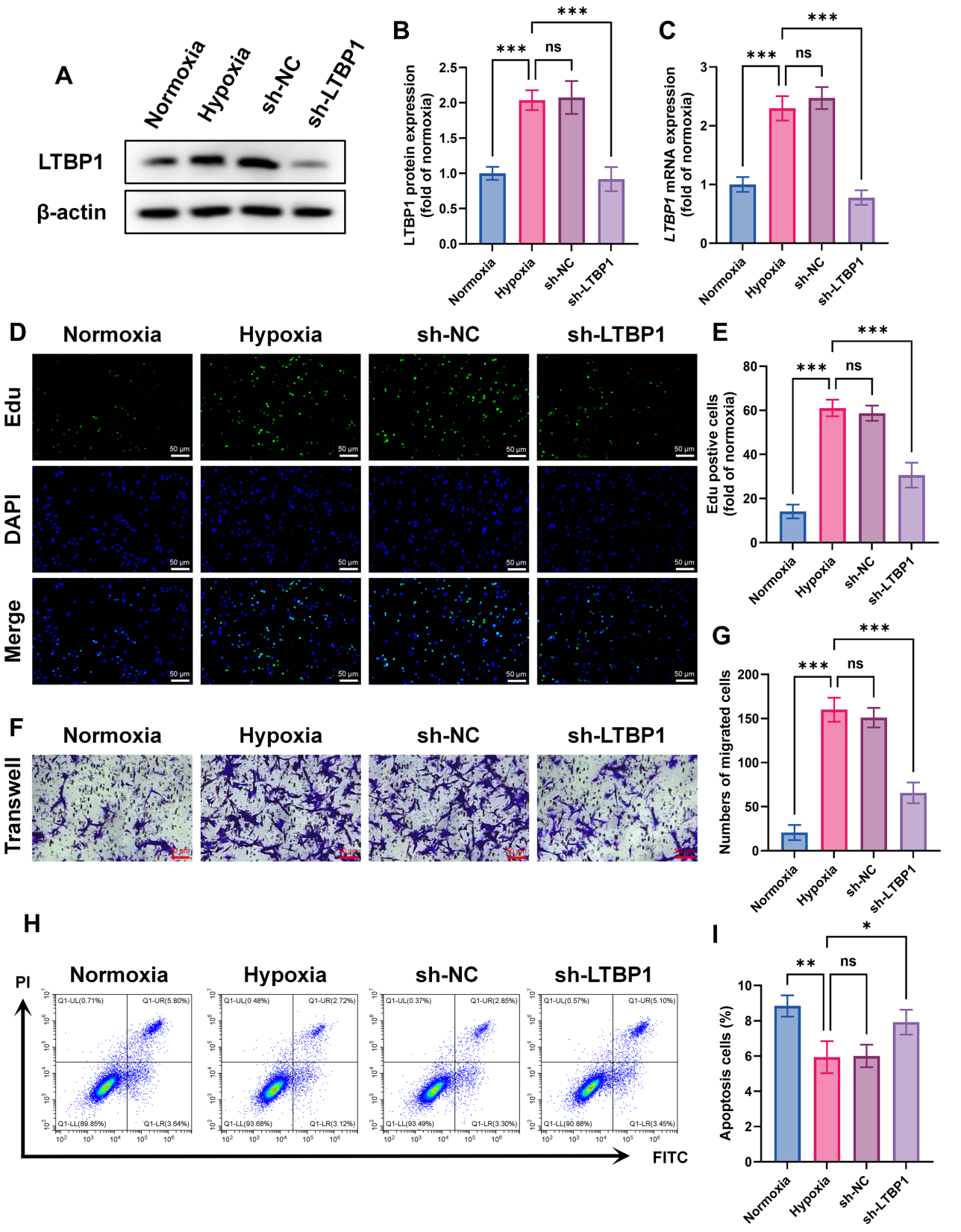


Fig. 4. LTBP1 depletion inhibits PASMC proliferation and migration and promotes apoptosis. (A–C) Validation of LTBP1 knockdown in PASMCs. (D,E) EdU incorporation assay for proliferation (scale bar: 50 μm). (F,G) Transwell assay for migration (scale bar: 50 μm). (H,I) Flow cytometric analysis of apoptosis using Annexin V/PI staining. n = 3 per group. ns, no significant difference, *$p < 0.05$, **$p < 0.01$, ***$p < 0.001$. PASMC, pulmonary arterial smooth muscle cell; EdU, 5-ethynyl-2′-deoxyuridine; PI, propidium iodide.

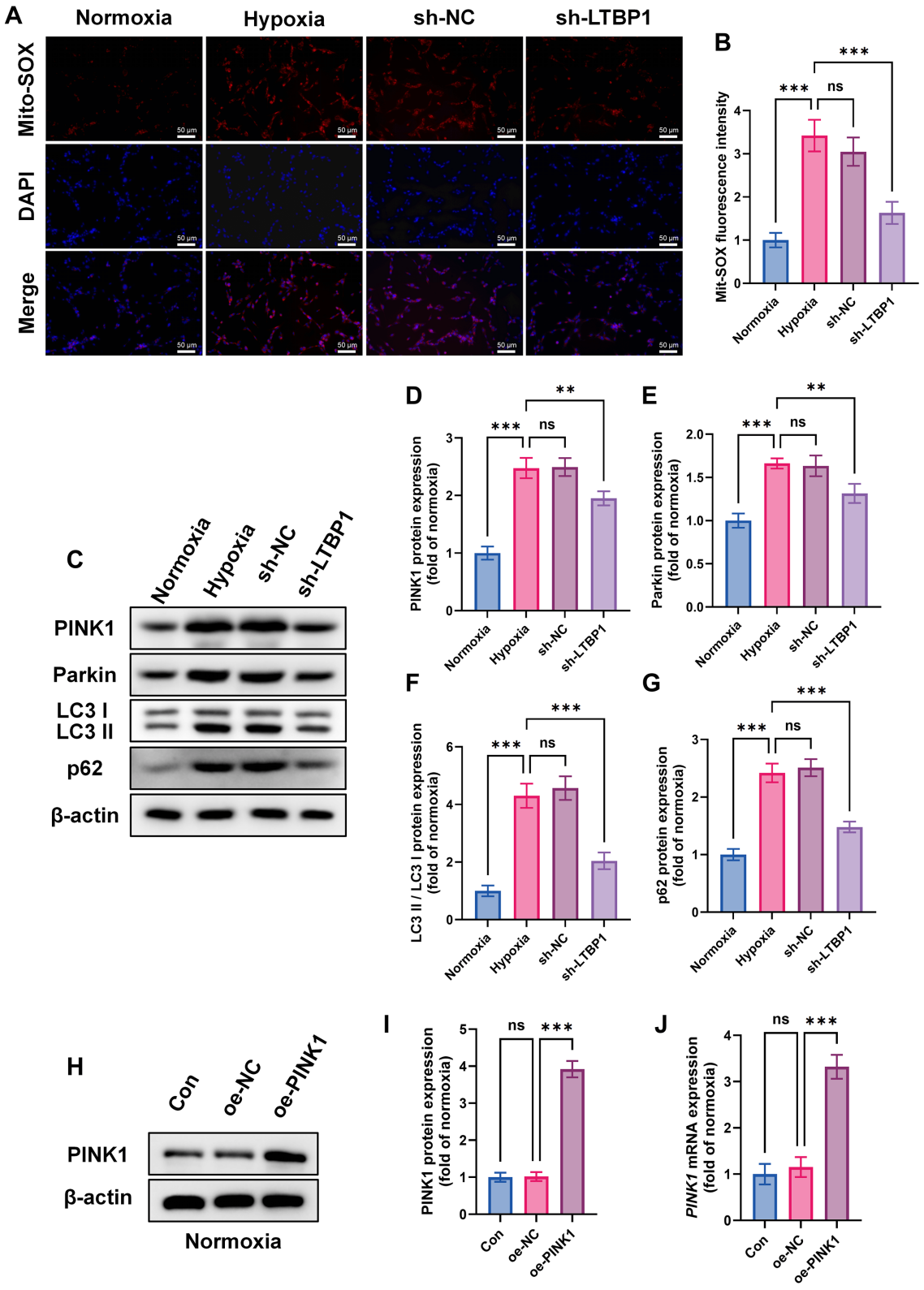


Fig. 5. LTBP1 regulates mitochondrial oxidative stress and mitophagy in PASMCs. (A) MitoSOX staining showing mitochondrial ROS levels (scale bar: 50 μm). (B) Quantitative analysis of MitoSOX fluorescence intensity. (C–G) Western blot analysis and quantification of mitophagy-related proteins. (H,I) Western blot analysis confirming PINK1 overexpression efficiency in PASMCs. (J) qPCR analysis confirming PINK1 overexpression at the mRNA level. n = 3 per group. ns, no significant difference, $^{**}p < 0.01$, $^{***}p < 0.001$. ROS, reactive oxygen species; qPCR, quantitative PCR.

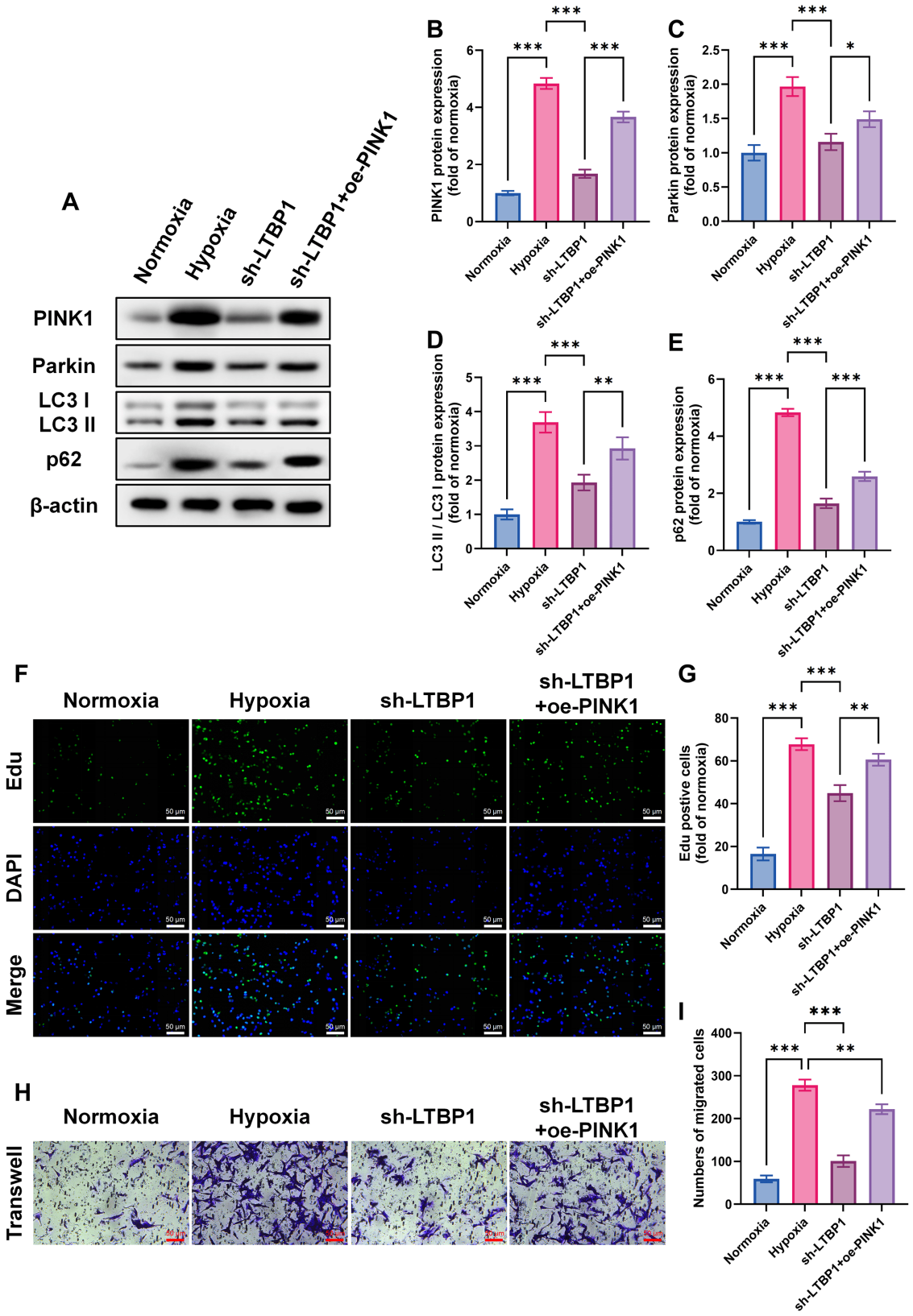


Fig. 6. PINK1 overexpression rescues mitophagy and cellular dysfunction induced by LTBP1 knockdown. (A–E) Western blot analysis and quantification of mitophagy-related proteins. (F,G) EdU proliferation assay (scale bar: 50 μm). (H,I) Transwell migration assay (scale bar: 50 μm). n = 3 per group. *$p < 0.05$, **$p < 0.01$, ***$p < 0.001$.

pression could partially reverse the suppressive effect of LTBP1 knockdown on PASMC proliferation (Fig. 6F), resulting in a markedly higher proportion of EdU-positive cells than the sh-LTBP1 group ($p < 0.05$) (Fig. 6G). Similarly, Transwell migration assays revealed that hypoxia markedly promoted PASMC migratory capacity ($p < 0.05$) (Fig. 6H), while LTBP1 depletion significantly suppressed cell migration ($p < 0.05$). This suppressive effect was partially rescued by PINK1 overexpression ($p < 0.05$), as indicated by a higher number of migrated cells in the sh-LTBP1+oe-PINK1 group compared with the sh-LTBP1 group (Fig. 6I). These findings suggest that restoration of PINK1-mediated mitophagy partially reverses the impact of LTBP1 silencing on PASMC proliferative and migratory behaviors, indicating that the effects associated with LTBP1 silencing may involve PINK1/Parkin-dependent mitophagy signaling.

Discussion

PAH is a fatal and progressively worsening cardiopulmonary condition, marked by sustained pulmonary vasoconstriction, vascular remodeling, and right ventricular dysfunction [3,27]. Increasing evidence has implicated mitochondrial dysfunction and impaired mitophagy in the development of PAH [10,28]. Our findings identify LTBP1 as a potential modulator of mitophagy-related signaling in PAH and demonstrate that LTBP1 contributes to pulmonary vascular remodeling and RV dysfunction, at least in part, through mechanisms that may involve PINK1/Parkin-associated signaling.

Through integrative bioinformatic analysis of the GSE117261 dataset, we identified 24 overlapping genes between DEGs and mitophagy-related genes, among which LTBP1 was significantly upregulated in PAH samples. LTBP1 is traditionally recognized as a key extracellular matrix (ECM)-associated protein that regulates the bioavailability and activation of TGF-β. Aberrant TGF-β signaling has been implicated in the development of vascular remodeling and fibrosis associated with PAH [29]. Our data provide additional evidence for a connection between LTBP1 and mitochondrial quality control, suggesting that LTBP1 may serve as a molecular bridge between ECM remodeling and intracellular mitochondrial homeostasis.

Mitochondrial dynamics and mitophagy are fundamental processes for maintaining cellular homeostasis, especially under stress conditions such as hypoxia [30]. The PINK1/Parkin pathway represents a well-characterized mechanism governing mitophagy, whereby damaged mitochondria are selectively recognized and removed [31]. The contribution of mitophagy to pulmonary hypertension appears to vary according to disease stage, cellular origin, and experimental models. In established PAH, reduced PINK1/Parkin-mediated mitophagy has been reported in patient-derived PASMCs, contributing to mitochondrial dysfunction and vascular remodeling [17]. In contrast, our study utilized a hypoxia-induced PASMC model to investigate early cellular responses to hypoxic stress. Consistent with previous studies using hypoxia-induced cellular models, our findings demonstrated that hypoxic stress triggered a mitophagy-related response in PASMCs [32,33]. In this study, hypoxic exposure significantly increased the expression of mitophagy-related proteins, including PINK1, Parkin, LC3 II/I, and p62, both in lung tissues and PASMCs, indicating activation of mitophagy signaling. Notably, LTBP1 knockdown markedly attenuated these changes, suggesting that LTBP1 positively modulates mitophagy-related signaling under hypoxic conditions.

At the cellular level, we demonstrated that LTBP1 promotes PASMC proliferation and migration while inhibiting apoptosis under hypoxic conditions. These phenotypic changes are hallmarks of pulmonary vascular remodeling and are critical drivers of PAH progression. Importantly, LTBP1 knockdown significantly suppressed these pathological behaviors, indicating that LTBP1 contributes to the pro-proliferative and anti-apoptotic phenotype of PASMCs. Mechanistically, these effects may be mediated through mitochondrial ROS accumulation and mitophagy-related signaling. Indeed, we observed that hypoxia-induced mitochondrial ROS production was significantly attenuated following LTBP1 silencing, suggesting that LTBP1 regulates oxidative stress and mitochondrial function.

Rescue experiments involving PINK1 overexpression were subsequently conducted to determine whether mitophagy contributes to the LTBP1-mediated effects. Notably, PINK1 overexpression partially counteracted the suppressive impact of LTBP1 silencing on mitophagy-related protein expression, PASMC proliferation, and migration. These findings provide direct evidence that the PINK1/Parkin pathway serves as an important downstream mediator of LTBP1 function. The partial nature of the rescue indicates that LTBP1 may exert its effects through mechanisms extending beyond the PINK1/Parkin axis. Given the established role of LTBP1 in extracellular matrix organization and TGF-β-related signaling, one possibility is that alterations in the extracellular matrix or TGF-β signaling may influence mitochondrial homeostasis through intermediate signals, such as integrin-mediated signaling, focal adhesion kinase (FAK)-dependent pathways, or other mechanotransduction mechanisms. These pathways may in turn affect mitochondrial ROS accumulation and mitophagy-related signaling in PASMCs.

This study has several limitations. First, while a regulatory relationship between LTBP1 and mitophagy exists, the precise molecular mechanisms linking LTBP1 to the PINK1/Parkin pathway remain unclear. Second, the assessment of autophagic flux was indirect, and future studies employing lysosomal inhibitors or tandem fluorescent reporters are needed to clarify whether LTBP1 directly affects

autophagic degradation. Third, while the hypoxia-induced mouse model recapitulates key features of PAH, validation in additional models, such as monocrotaline-induced PAH, would strengthen the generalizability of our findings.

Conclusions

This study identifies LTBP1 as a potential modulator of mitophagy-related signaling and pulmonary vascular remodeling in PAH. Our findings suggest that LTBP1 is associated with mitochondrial ROS accumulation and PINK1/Parkin signaling, and that LTBP1-associated effects may contribute to PASMC proliferation and migration while suppressing apoptosis. These results deepen the current understanding of PAH pathogenesis and indicate that targeting LTBP1-associated mitophagy signaling may represent a promising therapeutic strategy.

Availability of Data and Materials

The datasets used or analyzed during the current study are available from the corresponding author on reasonable request.

Author Contributions

XLZ and JWN designed the study and contributed to conceptualization and methodology. XLZ and JWN conducted data collection, investigation, data curation, validation, and formal analysis. XLZ drafted the original manuscript. JWN supervised the study and contributed to the review and editing of the manuscript. Both authors contributed to the critical revision of the manuscript for important intellectual content. Both authors have read and approved the final manuscript and agreed to be accountable for all aspects of the work.

Ethics Approval and Consent to Participate

All animal experiments were approved by the Animal Ethics and Welfare Committee of Wenzhou University (Approval No. WZU-2025-022) and were conducted in accordance with institutional guidelines and the international standards for animal care and use of laboratory animals, and the ARRIVE (Animal Research: Reporting of *In Vivo* Experiments) Guidelines 2.0.

Acknowledgment

Not applicable.

Funding

This work was supported by the Wenzhou Science and Technology Project (2022Y0370).

Conflict of Interest

The authors declare no conflict of interest.

References

[1] Guglielmi G, Dimopoulos K, Wort SJ. New therapies in pulmonary arterial hypertension: Recent insights. International Journal of Cardiology. Congenital Heart Disease. 2025; 19: 100571. https://doi.org/10.1016/j.ijcchd.2025.100571

[2] Flores CV, Chan SY. Therapeutic targets for pulmonary arterial hypertension: insights into the emerging landscape. Expert Opinion on Therapeutic Targets. 2025; 29: 327–343. https://doi.org/10.1080/14728222.2025.2507034

[3] Ghofrani HA, Gomberg-Maitland M, Zhao L, Grimminger F. Mechanisms and treatment of pulmonary arterial hypertension. Nature Reviews. Cardiology. 2025; 22: 105–120. https://doi.org/10.1038/s41569-024-01064-4

[4] Reinders S, Didden EM, Ong R. Survival, morbidity, and quality of life in pulmonary arterial hypertension patients: a systematic review of outcomes reported by population-based observational studies. Respiratory Research. 2024; 25: 373. https://doi.org/10.1186/s12931-024-02994-w

[5] Johnson S, Sommer N, Cox-Flaherty K, Weissmann N, Ventetuolo CE, Maron BA. Pulmonary Hypertension: A Contemporary Review. American Journal of Respiratory and Critical Care Medicine. 2023; 208: 528–548. https://doi.org/10.1164/rccm.202302-0327SO

[6] Li HR, Chen GL, Fang XL, Cai XJ, Xu RL, Li DD, et al. Circ_0068481 Affects the Human Pulmonary Artery Smooth Muscle Cells' Progression by miR-361-3p/KLF5 Axis. American Journal of Hypertension. 2024; 37: 33–45. https://doi.org/10.1093/ajh/hpad028

[7] Si M, Hu Y, Jin Z, Mao Y, Kang L. NF-κB and pulmonary hypertension: Advances in mechanistic research and therapeutic applications. American Heart Journal Plus: Cardiology Research and Practice. 2025; 60: 100669. https://doi.org/10.1016/j.ahjo.2025.100669

[8] Suliman HB, Nozik-Grayck E. Mitochondrial Dysfunction: Metabolic Drivers of Pulmonary Hypertension. Antioxidants & Redox Signaling. 2019; 31: 843–857. https://doi.org/10.1089/ars.2018.7705

[9] Riou M, Enache I, Sauer F, Charles AL, Geny B. Targeting Mitochondrial Metabolic Dysfunction in Pulmonary Hypertension: Toward New Therapeutic Approaches? International Journal of Molecular Sciences. 2023; 24: 9572. https://doi.org/10.3390/ijms24119572

[10] Zhang J, Yan H, Wang Y, Yue X, Wang M, Liu L, et al. Emerging insights into pulmonary hypertension: the potential role of mitochondrial dysfunction and redox homeostasis. Molecular and Cellular Biochemistry. 2025; 480: 1407–1429. https://doi.org/10.1007/s11010-024-05096-9

[11] Cartes-Saavedra B, Ghosh A, Hajnóczky G. The roles of mitochondria in global and local intracellular calcium signalling. Nature Reviews. Molecular Cell Biology. 2025; 26: 456–475. https://doi.org/10.1038/s41580-024-00820-1

[12] Xu X, Pang Y, Fan X. Mitochondria in oxidative stress, inflammation and aging: from mechanisms to therapeutic advances. Signal Transduction and Targeted Therapy. 2025; 10: 190. https://doi.org/10.1038/s41392-025-02253-4

[13] Chen C, Qin S, Song X, Wen J, Huang W, Sheng Z, et al. PI3K p85α/HIF-1α accelerates the development of pulmonary arterial hypertension by regulating fatty acid uptake and mitophagy. Molecular Medicine (Cambridge, Mass.). 2024; 30: 208. https://doi.org/10.1186/s10020-024-00975-9

[14] Liu R, Xu C, Zhang W, Cao Y, Ye J, Li B, et al. FUNDC1-mediated mitophagy and HIF1α activation drives pulmonary hypertension during hypoxia. Cell Death & Disease. 2022; 13: 634. https://doi.org/10.1038/s41419-022-05091-2

[15] Küng C, Lazarou M, Nguyen TN. Advances in mitophagy initiation mechanisms. Current Opinion in Cell Biology. 2025; 94: 102493. https://doi.org/10.1016/j.ceb.2025.102493

[16] Sarkar S, Chattopadhyay A, Bandyopadhyay D. Role of impaired mitochondrial dynamics and mitophagy in cardiovascular diseases: Possible therapeutic approaches. Life Sciences. 2025; 379: 123890. https://doi.org/10.1016/j.lfs.2025.123890

[17] Rehman R, Dieffenbach P, Vellarikkal SK, Corcoran AM, Pomales L, Arciniegas Rubio A, et al. PINK1/Parkin Deficiency Enhances Vascular Remodeling and Aggravates Hypoxia-induced Pulmonary Hypertension. American Journal of Respiratory Cell and Molecular Biology. 2025; 73: 859–870. https://doi.org/10.1165/rcmb.2024-0349OC

[18] Wang J, Zhang Y, Luo Y, Liu ML, Niu W, Li ZC, et al. PDK1 upregulates PINK1-mediated pulmonary endothelial cell mitophagy during hypoxia-induced pulmonary vascular remodeling. Molecular Biology Reports. 2023; 50: 5585–5596. https://doi.org/10.1007/s11033-023-08428-y

[19] Liu Y, Yi M, Wei H, Gu X, Liao W. Latent transforming growth factor beta binding protein 1 (LTBP1): roles as a multifunctional extracellular matrix regulator in human disease - from molecular mechanisms to clinical translation prospects. Folia Histochemica et Cytobiologica. 2026; 64: 1–25. https://doi.org/10.5603/fhc.110761

[20] Tubita A, Menconi A, Lombardi Z, Tusa I, Esparís-Ogando A, Pandiella A, et al. Latent-Transforming Growth Factor β-Binding Protein 1/Transforming Growth Factor β1 Complex Drives Antitumoral Effects upon ERK5 Targeting in Melanoma. The American Journal of Pathology. 2024; 194: 1581–1591. https://doi.org/10.1016/j.ajpath.2024.03.015

[21] Poonen-Honig I, Acosta AC, Sun M, Emerick V, Avila MY, Margo CE, et al. Latent-Transforming growth factor - β Binding protein 1 (LTBP1) in corneal stroma. Matrix Biology Plus. 2025; 28: 100185. https://doi.org/10.1016/j.mbplus.2025.100185

[22] Liu J, Zou Y, Wang J, Xu J. Exploration of common therapeutic targets for diabetic nephropathy and diabetic foot ulcers by integrated bioinformatics analysis and experimental validation. Molecular Biology Reports. 2025; 53: 192. https://doi.org/10.1007/s11033-025-11350-0

[23] Zhu T, Hu Q, Yuan Y, Yao H, Zhang J, Qi J. Mitochondrial dynamics in vascular remodeling and target-organ damage. Frontiers in Cardiovascular Medicine. 2023; 10: 1067732. https://doi.org/10.3389/fcvm.2023.1067732

[24] Zhang H, Tsui CK, Garcia G, Joe LK, Wu H, Maruichi A, et al. The extracellular matrix integrates mitochondrial homeostasis. Cell. 2024; 187: 4289–4304.e26. https://doi.org/10.1016/j.cell.2024.05.057

[25] Romanoski CE, Qi X, Sangam S, Vanderpool RR, Stearman RS, Conklin A, et al. Transcriptomic profiles in pulmonary arterial hypertension associate with disease severity and identify novel candidate genes. Pulmonary Circulation. 2020; 10: 2045894020968531. https://doi.org/10.1177/2045894020968531

[26] Lian G, You J, Lin W, Gao G, Xu C, Wang H, et al. Bioinformatics analysis of the immune cell infiltration characteristics and correlation with crucial diagnostic markers in pulmonary arterial hypertension. BMC Pulmonary Medicine. 2023; 23: 300. https://doi.org/10.1186/s12890-023-02584-4

[27] Li X, Liu P, Li Y, Liu Y, Hao W, Jin P, et al. Right Ventricular Fibrosis With Pulmonary Arterial Hypertension. Reviews in Cardiovascular Medicine. 2025; 26: 42395. https://doi.org/10.31083/RCM42395

[28] Gong C, Lan X, Xie Y, Wu X, Wu F, Chen X, et al. Overexpression of PRDX2 alleviates chronic thromboembolic pulmonary hypertension by modulating inflammation and mitophagy. Scientific Reports. 2025; 16: 1589. https://doi.org/10.1038/s41598-025-31063-5

[29] Huang Y, Ma W, Guo C, Su X. Mechanism of action and potential therapeutic targets of TGF-β-related signaling pathway and its downstream miRNA expression in pulmonary arterial hypertension. Frontiers in Pharmacology. 2025; 16: 1596767. https://doi.org/10.3389/fphar.2025.1596767

[30] Tian J, Mao Y, Liu D, Li T, Wang Y, Zhu C. Mitophagy in Brain Injuries: Mechanisms, Roles, and Therapeutic Potential. Molecular Neurobiology. 2025; 62: 10856–10868. https://doi.org/10.1007/s12035-025-04936-z

[31] Li S, Li X. Mitophagy in Hypertensive Cardiac Hypertrophy: Mechanisms and Therapeutic Implications. Journal of Clinical Hypertension (Greenwich, Conn.). 2025; 27: e70127. https://doi.org/10.1111/jch.70127

[32] Wang X, He Y, Li K, Xue Z, Li X, Xie M, et al. TRAF6 mediates vascular remodeling via endoplasmic reticulum stress-mitophagy in hypoxic pulmonary hypertension. Free Radical Biology & Medicine. 2026; 245: 237–249. https://doi.org/10.1016/j.freeradbiomed.2025.12.032

[33] Chen C, Xie Z, Ao D, Chen Y, Liu L, Li C. Transcription factor EB improves hypoxic pulmonary hypertension in fetal rats by suppressing NLRP3 inflammasome activation via induction of mitophagy. Scientific Reports. 2025; 15: 20356. https://doi.org/10.1038/s41598-025-07068-5